Polymorphous Crystallization and Multiple Melting Behavior of Poly(L-lactide): Molecular Weight Dependence

Pengju Pan, Weihua Kai, Bo Zhu, Tungalag Dong, and Yoshio Inoue*

Department of Biomolecular Engineering, Tokyo Institute of Technology, 4259-B-55 Nagatsuta, Midori-ku, Yokohama 226-8501, Japan

Received June 6, 2007; Revised Manuscript Received July 12, 2007

ABSTRACT: The effect of molecular weight (MW) on the polymorphous crystallization and melting behavior of poly(L-lactide) (PLLA) were systemically studied by differential scanning calorimetry (DSC), polarized optical microscopy (POM), wide-angle X-ray diffraction (WAXD), and time-resolved Fourier transform infrared (FTIR) spectroscopy. It was found that the polymorphism of PLLA is not influenced much by MW, and the α′- and α-form crystals are produced at low and high crystallization temperature (T_c), respectively, regardless of the MW. However, MW significantly affects the crystallization kinetics, and the crystallization rate reduces greatly with MW increasing. Moreover, the T_c- and MW-dependent melting behavior of PLLA was clarified with combining the DSC and FTIR results. It was found that the α′- to α-crystalline phase transition occurs prior to the dominant melting in both the low- and high-MW PLLA crystallized at low T_c. Unlike the high-MW PLLA, in low-MW PLLA crystallized at low T_c, the α′-form crystals only partially transform into the α-one, and some amounts of α′-form crystals melt directly without transition during the heating process. With increasing T_c, the melting of PLLA with various MWs changes from the phase transition + melting mechanism to the usual melt−recrystallization mechanism.

Introduction

Poly(L-lactide) (PLLA), well-known as a biodegradable and biocompatible thermoplastic among the family of environmentally friendly polymers, has attracted increasing attention in recent years because it is producible from renewable resources, such as corn, and nontoxic to the human body.[1] PLLA has been used in biomedical applications, such as surgical sutures, bone fixation devices, and controlled drug delivery systems. Furthermore, because of its favorable biodegradability, producibility from renewable resources, good mechanical properties, and versatile fabrication processes, it has excellent potential for substitution of petroleum-based polymers.[1]

Depending on the crystallization conditions, PLLA can crystallize in α-, *β*-, or *γ*-form.[2−4a] Crystallization of PLLA from the melt or solution under normal conditions results in its most common and stable polymorph, α-form, with a 10_3 helical chain conformation where two chains are interacting in an orthorhombic unit cell.[2a−c] The *β*-form was produced by stretching the α-form at very high drawing ratio and high temperature.[3] The *γ*-form, formed through epitaxial crystallization, was recently described by Cartier et al.[4a] Very recently, Zhang et al.[4b] reported that another disordered form, α′-form crystal, is likely to be produced in PLLA crystallized at low crystallization temperature (T_c).

The mechanical and thermal properties of a semicrystalline polymer greatly depend on the crystal structure and morphology. In addition, as for biodegradable polymers, their biodegradability is also influenced by the polymorphism.[5] So, it is quite important to control the polymorphism for optimizing the properties and production process of polymers. Recently, the crystallization process of PLLA has drawn much attention.[6−8] It has been found that the crystallization behavior of PLLA is very interesting and peculiar. The peculiar behavior is that the crystallization kinetics is discontinuous at 100−120 °C; that is, the curve of the half time in the melt−crystallization ($t_{1/2}$) vs T_c is discontinuous, and the profile of spherulite radius growth rate (G) vs T_c shows two peaks.[7] Some authors claimed that the discontinuity of PLLA crystallization kinetics resulted from the regime transition in this temperature range.[7]

On the other hand, the melting of semicrystalline thermoplastic is a very complex process, and it is influenced significantly by the crystallization conditions. Multiple melting peaks have been observed in many semicrystalline polymers, such as polypropylene (PP),[9a,b] polystyrene (PS),[9c] poly(ether ether ketone) (PEEK),[9d] poly(ethylene terephthalate) (PET),[9e] and some biodegradable polyesters.[10] Similarly, PLLA also shows the multiple melting peaks in the heating process, which quite depends on crystallization temperature. On the basis of the DSC measurements, the multiple melting behavior of PLLA was proposed to be due to the melt−recrystallization mechanism.[11] However, this interpretation has not been confirmed yet. Furthermore, as to the polymorphic polymers, the melting peaks are usually overlapped in the DSC curves, and in some cases it is impossible to reveal the actual melting mechanism only on the DSC results. As we know, FTIR is highly sensitive to the conformation and packing of polymers, making it widely used in the studies of the crystallization and melting behavior of polymers.[6a,b,12] Moreover, in the time-resolved FTIR spectroscopy, the characteristic bands can be correlated to the different crystal modifications and typically stay distinguishable over the course of melting. Therefore, it is considered that the complex melting behavior of PLLA can be probably well clarified with the aid of time-resolved FTIR spectroscopy.

As mentioned above, the crystallization kinetics and crystalline structure as well as the melting behavior of PLLA are quite dependent on the crystallization temperature. Besides T_c, the molecular weight (MW) is also one of the key variables governing the crystallization kinetics and polymorphism of polymers.[13] As a polymorphous polymer, it is considered that the polymorphic crystallization and melting behavior of PLLA

* To whom corresponding should be addressed: Tel +81-45-924-5794; Fax +81-45-924-5827; e-mail inoue.y.af@m.titech.ac.jp.

10.1021/ma071258d CCC: $37.00
Published on Web 08/18/2007

Table 1. Molecular Weight and Thermal Properties of PLLA Samples

code	M_n (kg/mol)	M_w (kg/mol)	M_w/M_n	T_g (°C)	T_{cc} (°C)	T_m (°C)	T_m^0 (°C)
PLLA15	15.4	21.3	1.38	48.0	83.2	160.9	174.2
PLLA41	40.7	64.5	1.58	55.9	104.1	170.2	185.0
PLLA118	118.3	176.6	1.49	59.1	113.9	176.5	192.4
PLLA219	218.6	359.2	1.64	59.7	122.4	173.4	197.6

is also probably dependent on MW. However, to our knowledge, the study on these aspects has not been reported systematically in the literature. In the present work, the polymorphic crystallization of PLLA with a wide range of MW under various conditions was investigated using DSC, POM, WAXD, and FTIR in detail. Moreover, to better understand the melting mechanism of PLLA, the time-resolved FTIR is used to monitor the T_c- and MW-dependent melting behavior of PLLA with combining the DSC measurements.

Experimental Section

Materials. PLLA samples with a number-average molecular weight (M_n) ranging from 15K to 219K were kindly supplied by Unitika Co. Ltd. (Kyoto, Japan). The M_n, weight-average molecular weight (M_w), and M_w/M_n for all the samples are tabulated in Table 1. Before use, all the samples were purified by precipitating into ethanol from chloroform solution, and then they were dried at 40 °C in a vacuum oven for 1 week.

Gel Permeation Chromatography (GPC). Molecular weight of the PLLA samples was measured on TOSOH HLC-8220 GPC system assembled with a VISCOTEK T-60AV viscometer. Chloroform was used as the eluent at a flow rate of 1.0 mL/min. TOSOH TSK standard polystyrene samples with the narrow molecular weight distribution were used as standards to calibrate the GPC elution curve.

Differential Scanning Calorimetry (DSC). The thermal properties of PLLA were measured by a Pyris Diamond DSC instrument (Perkin-Elmer Japan Co., Tokyo, Japan) equipped with a Perkin-Elmer intracooler 2P cooling accessory. The temperature and heat flow at different heating rates were calibrated using an indium standard with nitrogen purging. PLLA sample (6−8 mg) was weighed and sealed in an aluminum pan. In the cold-crystallization experiment, the melted samples were cooled at 100 °C/min to 0 °C after melting at 200 °C for 2 min, followed by a reheating to 200 °C at 10 °C/min. In the nonisothermal melt−crystallization experiment, the melted samples were cooled to 0 °C at 5 °C/min after melting in the same conditions. In the isothermal melt−crystallization experiment, the melted samples were cooled at a rate of 100 °C/min to the desired T_c after melting at 200 °C for 2 min and allowed to crystallize at T_c. Subsequently, they were heated to 200 °C at 10 °C/min (or 2 °C/min) to register the melting curve. As for the PLLA samples crystallized at 90 °C ≤ T_c ≤ 130 °C, the isothermal melt−crystallization time is 60 min. For the samples crystallized at T_c > 130 °C and T_c < 90 °C, the isothermal melt−crystallization time is 240 min. These times were found to be enough to finish the crystallization of all the PLLA samples.

Polarized Optical Microscopy (POM). POM observation was performed on an Olympus BX90 polarizing optical microscopy (Olympus Co., Tokyo, Japan) equipped with a digital camera. The sample was placed between two glass slides and heated to 200 °C in a hot stage (Mettler FP82HT), where the sample remained for 2 min. Then, the sample was quenched to the desired T_c for crystallization. The sizes of growing spherulites were monitored by taking microphotographs during appropriate time intervals before the spherulites impinged. Plotting the spherulite radius against the growth time, a straight line was obtained, and the slope was considered as its average radial growth rate.

Wide-Angle X-ray Diffraction (WAXD). WAXD analysis was carried out on a Rigaku RU-200 (Rigaku Co., Tokyo, Japan), working at 40 kV and 200 mA, with Ni-filtered Cu Kα radiation (λ = 0.154 18 nm). Scans were made between Bragg angles of 5°−50° at a rate of 1°/min.

FTIR Spectroscopy. The FTIR measurements were performed on an FTIR-6100 spectrometer (JASCO, Japan) equipped with an IMV-4000 multichannel infrared microscope (JASCO, Japan) and a MCT detector in the transmission mode. PLLA sample was placed between two pieces of BaF_2 slides, and then it was melted at 200 °C for 2 min before quenched to the desired T_c. For studying the crystalline structure, all crystallized samples were measured at 23 °C to erase the temperature effect on the IR spectra. For studying the melting behavior, after the melt−crystallization the sample was heated from T_c to 190 °C at 2 °C/min in a LK-600FTIR hot stage (Japan High Tech Co., Ltd.). The FTIR spectra were recorded at a 1 °C interval during the heating process, and the spectra were collected with 64 scans and a resolution of 2 cm^{-1}.

Results and Discussion

Crystallization Kinetics. Figure 1a shows the DSC heating scans of the quenched PLLA samples at a rate of 10 °C/min. In addition to the glass transition, all of the curves show an exothermic cold-crystallization peak and an obvious melting peak at higher temperature. The values of glass transition temperature (T_g), cold crystallization temperature (T_{cc}), melting temperature (T_m), and equilibrium melting temperature (T_m^0), which was obtained by the Hoffman−Weeks procedure,[14] are listed in Table 1. The values of T_g, T_m, and T_m^0 of all the PLLA samples are quite dependent on the molecular weight. The T_g, T_m, and T_m^0 of PLLA219 are more than 10 °C higher than those of PLLA15. With increasing MW, the cold crystallization peak shifts to higher temperature, owing to the drop of the crystallization rate.

The DSC curves of PLLA registered during the melt−crystallization at a cooling rate of 5 °C/min are depicted in Figure 1b. With decreasing MW, the crystallization peak shifts to higher temperature and also becomes much sharper, indicating that the crystallization rate increases with the decrease of MW. When the MW is more than 118K, the crystallization of PLLA cannot be finished during the cooling process. Besides, as for PLLA15, a small peak shoulder is present at 100−120 °C prior to the dominant crystallization peak, as indicated by the arrow. This signifies that the crystallization mechanism possibly changes in this temperature region.[7b]

In order to study the effect of T_c on the crystallization behavior, the isothermal crystallization of PLLA with various MWs were also measured using DSC. The time corresponding to the crystallization peak (t_p) of the isothermal DSC curves was plotted as a function of T_c for each PLLA sample, and the results are shown in Figure 2a. All t_p-T_c curves show a minimum at 90−110 °C, indicating that the crystallization is fastest at this temperature region. It should be noted that for all the PLLA samples $T_c \approx 110$ °C is a critical temperature in the t_p-T_c curves, and the t_p value increases suddenly nearby this critical temperature. Moreover, this critical temperature is almost not affected by MW.

The spherulite radius growth rate (G) of PLLA with various MWs was also evaluated using POM, and the G value is plotted as a function of T_c in Figure 2b. Generally, the difficulty in nucleation at low undercooling and the poor diffusivity at high undercooling lead to the bell-shaped growth rate dependence on T_c for the crystallization of polymers. Nevertheless, the

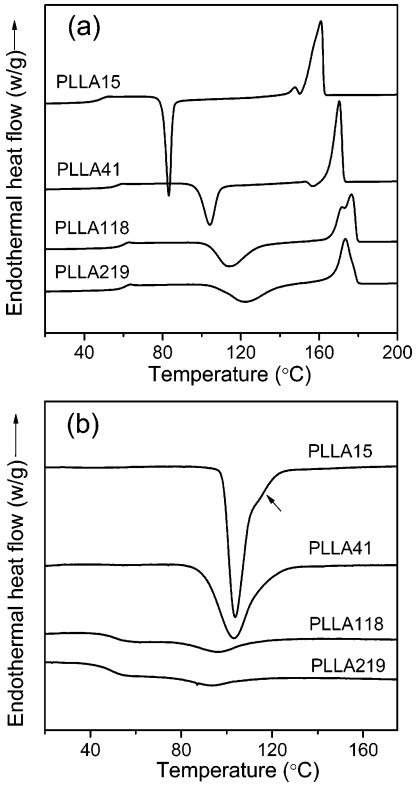

Figure 1. DSC thermograms of (a) cold crystallization at a heating rate of 10 °C/min and (b) nonisothermal melt−crystallization at a cooling rate of 5 °C/min for PLLA with various MWs.

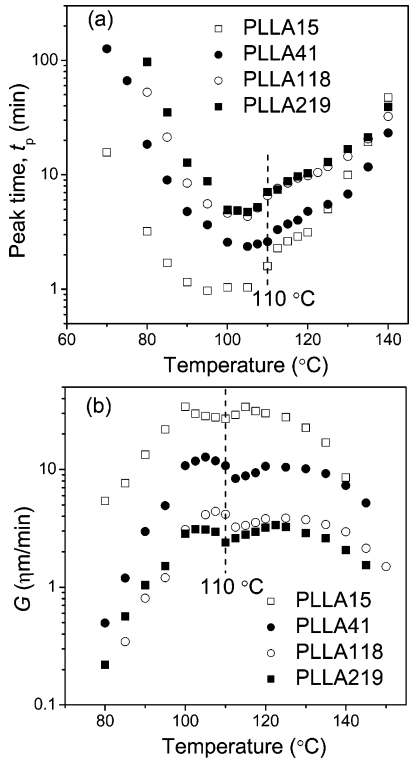

Figure 2. (a) Peak time (t_p) and (b) spherulite radius growth rate (G) of PLLA with various MWs as a function of T_c.

crystalline growth behavior is very unusual for all the PLLA samples. The G value shows a bimodal T_c dependence, with a minimum located at nearby 110 °C between two peaks, and this T_c dependence is very similar to the results shown in Figure 2a. The minimum is almost not influenced by MW. Usually, because of the different growth kinetics, the presence of more

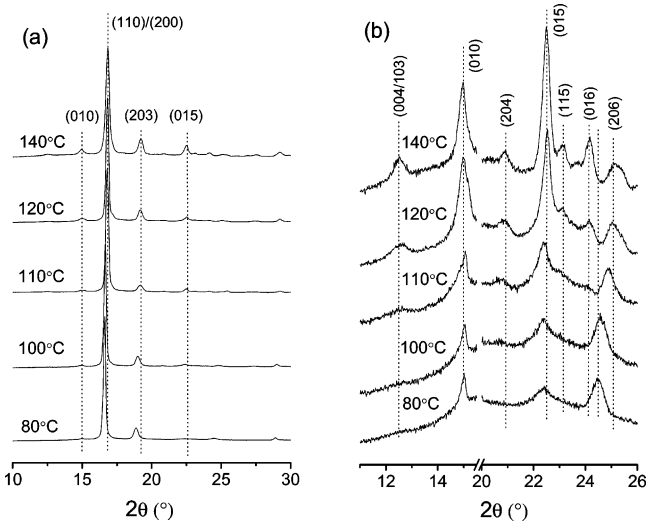

Figure 3. (a) WAXD patterns and (b) enlarged WAXD patterns of PLLA15 isothermally melt-crystallized at T_c = 80−140 °C.

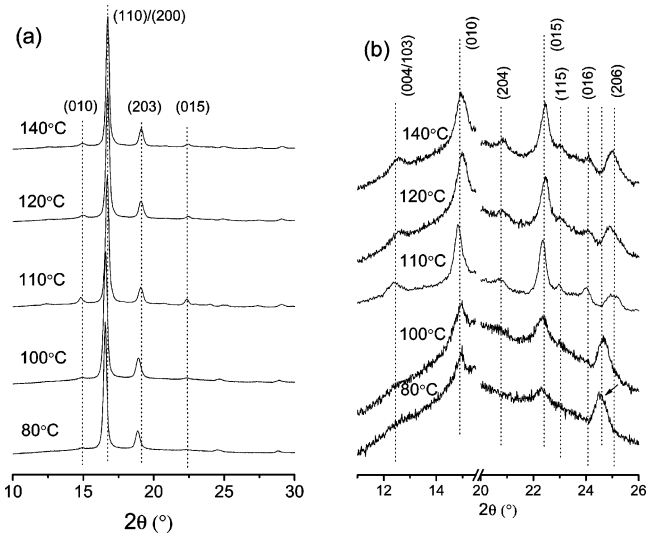

Figure 4. (a) WAXD patterns and (b) enlarged WAXD patterns of PLLA219 isothermally melt-crystallized at T_c = 80−140 °C.

than one crystallographic form usually causes the multipeaked spherulite growth kinetics.[10a]

As shown in Figures 1 and 2, the crystallization kinetics are strongly dependent on the MW of PLLA. With decreasing MW, the T_g and T_m^0 values decrease, especially for the lower MW samples (MW < 118K). Generally, the intrinsic viscosity of polymer drops greatly with the decrease of MW, which is usually in an exponential relationship.[15] Therefore, as MW decreases, the mobility of polymer chains will be improved, inducing the much easier diffusion of polymer chains during the crystallization process. Accordingly, the lower MW samples show much faster crystallization rate than those of the higher MW ones. On the other hand, as for higher MW samples (MW ≥ 118K), with the decrease of MW, the mobility of polymer chains increases little due to the exponential relationship between MW and intrinsic viscosity.[15] Consequently, the crystallization rate increases little with decreasing MW for the PLLA samples, the MW of which is larger than 118K.

Crystalline Structure. The crystalline structure of PLLA melt-crystallized at different T_cs was investigated by WAXD, and the results for PLLA15 and PLLA219 are shown in Figures 3 and 4, respectively. As for both PLLA15 and PLLA219, notable differences in the WAXD patterns are observed between

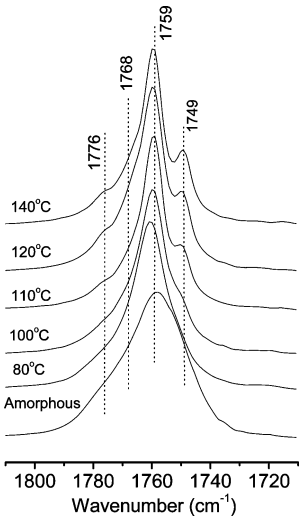

Figure 5. IR spectra in the 1810−1710 cm^{-1} region of amorphous and crystalline PLLA15 isothermally melt-crystallized at T_c = 80−140 °C.

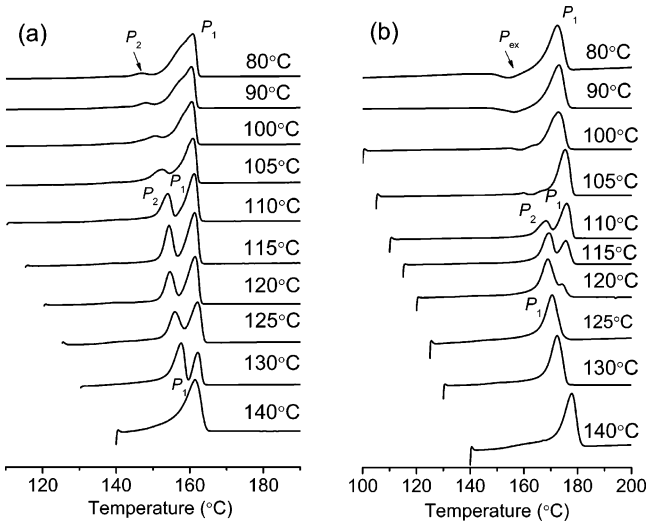

Figure 6. DSC heating curves of (a) PLLA15 and (b) PLLA118 isothermally melt-crystallized at various T_cs.

the samples crystallized at low and high T_c. The major differences are as follows: (1) compared to the samples crystallized at high T_c, the samples crystallized at low T_c show two dominant diffraction peaks, that is, 110/200 and 203 reflections, at lower 2θ; (2) the samples crystallized at high T_c show some small diffraction peaks at 2θ = 12.5°, 20.8°, 23.0°, 24.1°, and 25.1°, which have been assigned to the reflections of 004/103, 204, 115, 016, and 206 planes,[6c] respectively, whereas the samples crystallized at low T_c do not show these peaks; (3) the peak appeared at 2θ = 24.6° (indicated by the arrow) is characteristic of the samples prepared at low T_c, and it disappears at high T_c. Besides, as regards PLLA41 and PLLA118, very similar T_c-dependent WAXD patterns (data not shown) were observed.

Figure 5 depicts the IR spectra of the C═O stretching band (1810−1710 cm^{-1}) for PLLA15 melt-crystallized at different T_cs. Similar to the IR spectra of PLLA with higher MW,[4b] the IR spectra of low-MW PLLA samples crystallized at high and low T_c are significantly different. First, in the ν(C═O) region, besides the dominant band (1759 cm^{-1}), three new bands are observed at 1749, 1768, and 1776 cm^{-1}. These three new bands are distinct in the PLLA crystallized at high T_c. However, these bands are so weak that they cannot be clearly observed in the PLLA crystallized at low T_c. Also, with increasing T_c, the dominant band, 1759 cm^{-1} band, shifts toward lower wavenumber side by about 1 cm^{-1}.

For all the PLLA samples, the WAXD and IR data are consistent very well with each other. The characteristics of the WAXD patterns and IR spectra of the PLLA samples crystallized at high T_c are the same as those of the PLLA α-form crystal,[3d,16] indicating that only the α-form crystal is produced at high T_c for all the PLLA samples with both low- and high-MW. Both the WAXD patterns and IR spectra are obviously different for all the PLLA samples crystallized at high and low T_c, confirming that another crystal form, that is, the α′-form, was mainly produced at low T_c in all the PLLA samples. According to Zhang et al.,[4b] both the α′- and α-form crystals have the same 10_3 helix chain conformation and orthorhombic unit cell, but the packing of the side groups in the helical chains of the α′-form crystal is less ordered and looser than that of the α-form crystal. The viscosity of crystallization system is higher at lower T_c, which possibly makes the structural adjustment and diffusion of polymer chains more difficult. It is much difficult for the various functionalities, especially the side groups, to reach the ideal stable state with the lowest packing energy. Accordingly, the less ordered one, that is, the α′-form crystal, is mainly developed at lower T_c. What is more, for all the PLLA samples with different MWs, 100−120 °C is the critical temperature region for the formation of the α′- and α-form crystals, where the mixture of α′- and α-form crystals is developed. Furthermore, the crystallization kinetics also change discontinuously at this temperature region for all the PLLA samples, as shown in Figure 2. Because the different crystal modifications usually have the different crystallization kinetics, it is reasonable to consider that the discontinuousness of crystallization kinetics is due to the polymorphism of PLLA. The different crystallization kinetic between T_c < 110 °C and T_c > 110 °C might be mainly resulted by the different nucleation or growth mechanisms between the α′- and α-form crystals.

DSC Measurements on the Melting Processes. Figure 6 shows the DSC thermograms at a heating scan rate of 10 °C/min observed for PLLA15 and PLLA118 crystallized at T_c = 80−140 °C. Clearly, the melting behavior of PLLA is strongly dependent on T_c. As for PLLA with high-MW (PLLA118), when T_c < 105 °C, a small exotherm (donated as P_{ex}) appears prior to the dominant melting peak (P_1), as shown in Figure 6b. However, at 110 °C < T_c < 125 °C, the small exotherm disappears, and two endotherms (P_1 and P_2) are present. At T_c > 125 °C, only one endotherm (P_1) appears. As regards PLLA41 and PLLA219, the very similar T_c-dependent DSC curves were observed (data not shown), so the melting of PLLA118 was only examined as an example of high-MW PLLA samples in this study. Nevertheless, as shown in Figure 6a, the melting of PLLA15 is considerably different from the other samples with higher MW. The dissimilarity mainly focuses on the samples crystallized at low T_c. Rather than the exotherm, a small and broad endotherm (P_2) is present prior to the dominant melting peak for PLLA15 crystallized at T_c < 105 °C.

So far, three main mechanisms, namely, melt−recrystallization, dual (or multiple) lamellae population, and dual (or multiple) crystal structure, have been proposed to explain the multiple melting behavior of polymers.[11b] The melt−recrystallization mechanism suggests that the low- and high-temperature endotherms in the DSC curve can be attributed respectively to the melting of original crystals and that of crystals formed through the melt−recrystallization process during the heating scan. The dual (or multiple) lamellae population mechanism

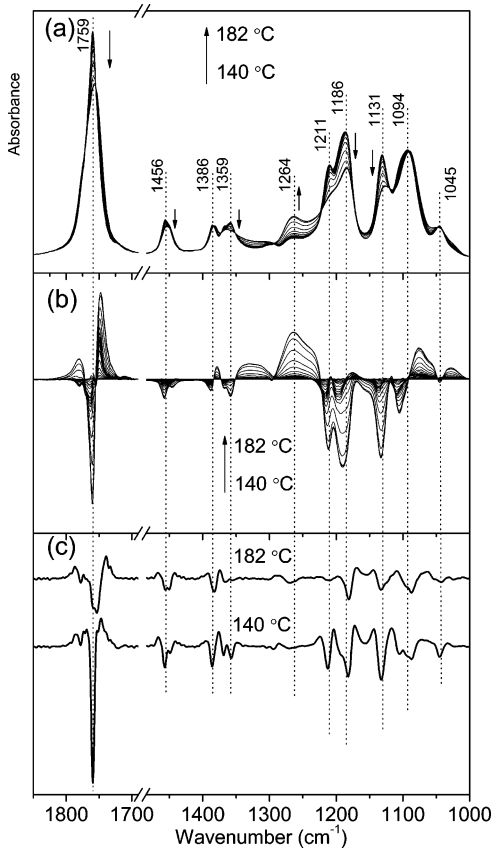

Figure 7. (a) Temperature-dependent IR spectra, (b) difference spectra calculated by subtracting the initial crystalline spectra (at 140 °C), in the 1850−1000 cm^{-1} range for PLLA118 isothermally melt-crystallized at T_c = 80 °C registered in the heating process at a rate of 2 °C/min from 140 to 182 °C. (c) Second derivatives of the spectra collected before (at 140 °C) and after (at 182 °C) melting.

associates the multiple melting with the different morphologies formed prior to the heating scan, for example, from the primary and secondary crystallization. In the case of polymorphic polymer, the existence of different crystal structures may also lead to the appearance of multiple melting peaks. As shown in Figure 6, the T_c- and MW-dependent melting of PLLA is so complex that it is difficult to distinguish which mechanism is reasonable, only according to the DSC results. Therefore, the DSC data will be further analyzed in combination with the FTIR results as shown below.

In Situ Observation on Polymorphic Melting of High-MW PLLA. In order to clarify the complex T_c- and MW-dependent melting behavior, the melting process of PLLA samples melt-crystallized at various T_cs was simultaneously surveyed by time-resolved FTIR spectroscopy. Figure 7a shows the temperature-dependent IR spectra in the 1850−1000 cm^{-1} range collected in the heating process at 2 °C/min for the high-MW PLLA (PLLA118) crystallized at T_c = 80 °C. The difference spectra, which were obtained by subtracting the initial spectra of the crystalline sample collected at 140 °C, are shown in Figure 7b. Also, the second derivatives of the FTIR spectra registered at 140 °C (before melting) and 182 °C (after melting) were calculated, which are presented in Figure 7c. Obviously, the stretching band of the C═O group (1850−1700 cm^{-1}) and the bands at 1300−1000 cm^{-1} are very sensitive to the melting process. However, the bands at 1300−1000 cm^{-1}, which are induced by ν(C−O−C), $\gamma(CH_3)$, ν(C−CH_3), and their coupling vibration,[12a] are heavily overlapped. Besides, the ν(C═O) bands are greatly sensitive to the crystalline structure of PLLA, as

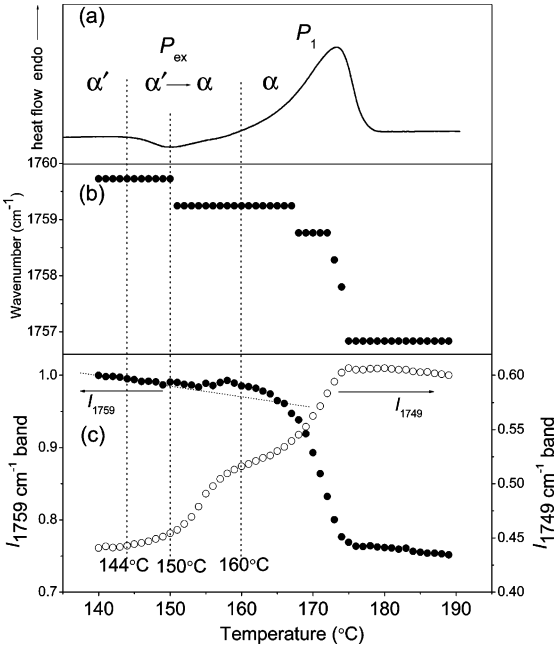

Figure 8. (a) DSC heating curve, temperature-dependent (b) wavenumber of the C═O stretching band, and (c) normalized intensity of the 1759 and 1749 cm^{-1} bands for PLLA118 isothermally melt-crystallized at T_c = 80 °C during the heating process at a rate of 2 °C/min.

shown in Figure 5. Accordingly, the ν(C═O) bands are mainly evaluated here.

As for PLLA118 melt-crystallized at T_c = 80 °C, the temperature-dependent wavenumber of the ν(C═O) band is shown in Figure 8b. All the IR spectra collected at different temperatures were normalized by the absorbance of 1759 cm^{-1} band registered at the initial temperature, and the normalized intensities of the 1759 cm^{-1} (I_{1759}) and 1749 cm^{-1} (I_{1749}) bands as a function of temperature are presented in Figure 8c. The corresponding DSC heating curve is also shown in Figure 8a. As shown in Figure 8a, the melting process consists of two parts in the DSC curve, that is, the exotherm P_{ex} and the big endotherm P_1. For comparison, in Figure 9 the temperature-dependent FTIR spectra in the region 1800−1720 cm^{-1} are separately illustrated in two groups according to the temperature region, that is, 144−160 and 162−180 °C, which are in parallel with the temperature regions of the two DSC peaks, P_{ex} and P_1, respectively.

Three major features should be addressed for Figure 8. First, the I_{1759} value shows a distinct deviation from the linear change above 150 °C, and especially when the temperature reaches nearby 155 °C, the increase of I_{1759} can be clearly observed. Second, as shown in Figure 8c, with increasing temperature the I_{1749} value increases greatly at 144−160 °C, which corresponds to the temperature region of P_{ex} in the DSC curve. These can also be observed distinctly in Figure 9a. Furthermore, the increase of I_{1749} becomes much drastic at 150−160 °C. At T > 160 °C, because of the increase of the content of the amorphous phase, the ν(C═O) band shifts toward lower wavenumber side with increasing temperature (see Figure 9b), resulting in the increase of I_{1749}. Third, as shown in Figure 8b, it should be noted that the peak shift to lower wavenumber of ν(C═O) band was also observed nearby 150 °C prior to the dominant melting.

As shown in Figure 5, the band at 1749 cm^{-1}, which appears only in the spectra of the samples crystallized at higher T_c, is the characteristic of PLLA α-form crystal. Therefore, the increase of I_{1749} at 144−160 °C, where the exotherm (P_{ex}) is

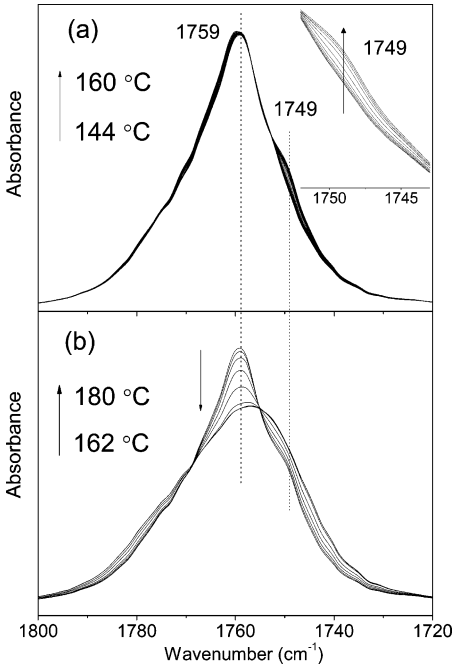

Figure 9. Temperature-dependent IR spectra in the 1800−1720 cm^{-1} range for PLLA118 isothermally melt-crystallized at T_c = 80 °C registered in the heating process at 2 °C/min from (a) 144 to 160 °C and (b) 162 to 180 °C.

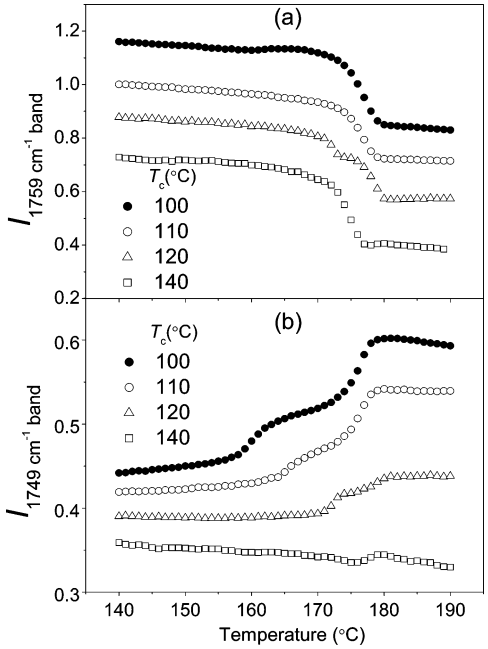

Figure 10. Temperature-dependent normalized intensity of the (a) 1759 and (b) 1749 cm^{-1} bands for PLLA118 isothermally melt-crystallized at T_c = 100, 110, 120, and 140 °C during the heating process at a rate of 2 °C/min.

observed in the DSC heating curves, indicates the formation of the α-form crystal in this temperature region. These strongly suggest that the α′- to α-crystalline phase transition occurs prior to the major melting. In addition, the ν(C═O) band of the α′-form crystal locates at higher wavenumber than that of the α-form crystal. Accordingly, the wavenumber shift of the ν-(C═O) band at 144−160 °C also confirms the conclusion that the α′- to α-crystalline phase transition takes place before the dominant melting. Moreover, the chain packing of the α′-form crystal is looser and less ordered, so it seems that the α′-form crystal has a lower density as compared to the α-form crystal. The intensity of IR bands for the α′-form crystal is likely to be lower than that of the α-form crystal. Therefore, owing to the α′- to α-crystalline phase transition, the I_{1759} value increases in the temperature range 144−160 °C. The α-form crystal developed during the transition process melts at higher temperature, leading to a P_1 endotherm in the DSC curve.

Because no clear evidence on the melting of the α′-form crystal at 144−160 °C is observed in the DSC and FTIR results, the α′- to α-crystalline phase transition can be the direct solid−solid phase transition or the indirect one where the melting of the unstable phase and the recrystallization of the stable phase take place synchronously. The latter is more frequently observed near the melting point of the polymorphous polymers during the heating process.[9a,10a] As for high-MW PLLA, the temperature region for the phase transition is nearby 150 °C (see Figure 8a), which is about 40 °C lower than the T_m^0. Because of the larger undercooling (T_m^0-T), almost all the melted α′-form crystal can be possibly recrystallized into the α-form crystal synchronously in the heating process. In this case, the two processes, that is, the melting of α′-form crystal and the recrystallization of α-form crystal, can be considered as one process, that is, the α′- to α-crystalline phase transition. In other words, for the high-MW PLLA crystallized at 80 °C, it seems that almost all the α′-form crystal transforms into the α one during the heating scans.

To study the effect of T_c on the melting process, the melting of PLLA118 crystallized at T_c = 100, 110, 120, and 140 °C were investigated using time-resolved FTIR spectroscopy. The intensities of the 1759 and 1749 cm^{-1} bands are plotted as a function of temperature in parts a and b of Figure 10, respectively. The intensity was normalized by the same procedure as that used in Figure 8c. For clarity, the curves shown in Figure 10 were shifted arbitrarily in the vertical direction. For PLLA118 crystallized at T_c = 100 °C, the I_{1759} and I_{1749} values have the very similar tendency of variation as those of PLLA118 crystallized at T_c = 80 °C, indicating that the α′- to α-crystalline phase transition occurs before melting. As for PLLA118 crystallized at T_c = 110 and 120 °C, the increase of I_{1759} disappears, but the I_{1749} value still increases with temperature before the dominant melting. However, the extent of the increase in I_{1749} is much weaker than that of PLLA118 crystallized at T_c = 80 and 100 °C. The results suggest that some amounts of the α′-form crystals are also produced in these conditions, and it transforms into the α-one in the heating scan. Combining the DSC and IR results, at T_c = 110−120 °C, the seeming endotherm at lower temperature (P_2) is contributed by two processes, that is, the α′- to α-crystalline phase transition and the melting of the original α-form crystal. The endotherm at higher temperature, P_1, arises from the melting of the α-form crystal formed in (i) its own melting−recrystallization process and (ii) the α′- to α-crystalline phase transition process. As regards the PLLA118 crystallized at T_c = 140 °C, no increase of the I_{1749} value before the melting is observed, and also the I_{1759} value decreases monotonously in the heating process. These signify that the unique DSC melting peak P_1 of PLLA crystallized at high T_c is attributed to the direct melting of the α-form crystal.

In Situ Observation on Polymorphic Melting of Low-MW PLLA. For low-MW PLLA (PLLA15) isothermally melt-crystallized at 80 °C, the intensities of 1759 cm^{-1} (I_{1759}) and 1749 cm^{-1} (I_{1749}) bands, which were normalized by the absorbance of 1759 cm^{-1} band collected at the initial temperature, are shown as a function of temperature in Figure 11b.

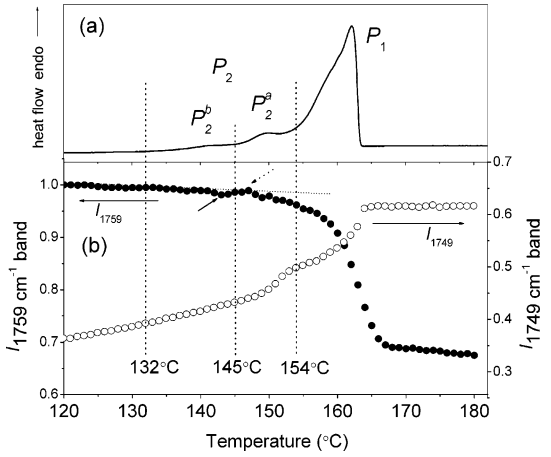

Figure 11. (a) DSC heating curve and (b) temperature-dependent normalized intensity of the 1759 and 1749 cm^{-1} bands for PLLA15 isothermally melt-crystallized at $T_c = 80$ °C during the heating process at a rate of 2 °C/min.

The corresponding DSC heating curve is illustrated in Figure 11a for comparison. As regards PLLA15 crystallized at low T_c, one broad endotherm (denoted as P_2) is present prior to the dominant melting peak, as shown in Figure 11a. It seems that the broad endothermic peak consists of two parts, which are denoted as P_2^a (145−154 °C) and P_2^b (132−145 °C). Besides, as shown in Figure 11b, the $I_{1759}-T$ curve of PLLA15 is different from that of PLLA118. In the case of PLLA15, the change of I_{1759} value observed in the temperature range 132−154 °C is very complex. It should be noted that when the temperature reaches 140 °C, with the increase of temperature the I_{1759} value first decreases (indicated by the solid arrow) and then it increases nearby 145 °C (indicated by the dashed arrow). Besides, at $T < 145$ °C, the I_{1749} value increases gradually during the heating process. However, the increase of the I_{1749} value becomes much sharper at 145−154 °C.

As described above, only the α′-form crystal was produced in PLLA15 crystallized at $T_c = 80$ °C. Therefore, some amounts of α′-form crystals seem to melt in the temperature region corresponding to the endotherm P_2, which can be confirmed by the decrease of the I_{1759} value nearby 140 °C (indicated by the solid arrow in Figure 11b). On the other hand, the sharp increase of the I_{1749} value with temperature in the range 145−154 °C strongly suggests that the α-form crystal is formed in the temperature region corresponding to P_2, especially in the 145−154 °C range. This conclusion is also supported by the phenomena that the I_{1759} value increases nearby 145 °C (indicated by the dashed arrow in Figure 11b). According to Yamamoto et al.,[9a] the *β*-form crystal of isotactic polypropylene (iPP) shows the very similar melting behavior as that of the PLLA α′-form crystal. Using the deconvolution analyses of the DSC profiles, they found that the temporary melting of the iPP *β*-form crystal and the synchronized recrystallization into the α-form crystal occur before the final melting. On basis of the DSC and FTIR results, it is reasonable to consider that the endotherm P_2 includes two contributions, that is, (i) the melting of the initial α′-form crystal and (ii) the recrystallization into the α-form crystal from the melted α′-form crystal, which result in the endotherm and exotherm in the DSC curve, respectively. Because of the overlapping of the endotherm and exotherm, the resulted DSC melting curve becomes more complex, as shown in Figure 11a. The dominant endotherm, P_1, is likely to arise from the melting of the α-form crystal formed in the phase transition process.

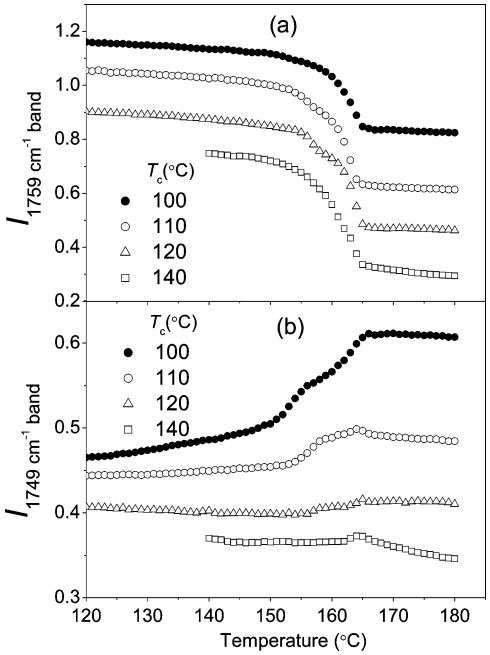

Figure 12. Temperature-dependent normalized intensity of the (a) 1759 and (b) 1749 cm^{-1} bands for PLLA15 isothermally melt-crystallized at $T_c = 100$, 110, 120, and 140 °C during the heating process at a rate of 2 °C/min.

However, it is notable that the melting of low- and high-MW PLLA crystallized at low T_c is considerably different, even though the α′-form crystal is produced in both samples. This difference is probably resulted by the crystallization kinetics. In the case of low-MW PLLA, the temperature region for phase transition is nearly 145 °C (see Figure 11a), which is only about 30 °C lower than the T_m^0. Under this smaller undercooling (T_m^0-T), it seems that the melted α′-form crystal cannot be recrystallized into the α-form crystal synchronously during the heating scan due to the smaller recrystallization rate of the α-form crystal. Finally, the α′-form crystals transform only partially into the α-one, and some amounts of α′-form crystals melt directly during the heating scans. Besides, another plausible explanation is that, due to the high mobility of polymer chains, the as-produced α′-form crystal in the low-MW sample is more perfect than that in the high-MW one. As a result, some perfect α′-form crystals melt directly without transition during the heating process.

Figure 12 shows the normalized intensity of the 1759 and 1749 cm^{-1} bands as a function of temperature for PLLA15 crystallized at $T_c = 100$, 110, 120, and 140 °C. As for PLLA15 crystallized at $T_c = 100$ °C, the temperature dependences of the I_{1759} and I_{1749} values are very similar to those of the sample crystallized at $T_c = 80$ °C, signifying that (i) the melting of the α′-form crystal and (ii) the recrystallization into the α-form crystal from the melted α′-form crystal occur simultaneously prior to the dominant melting. For PLLA15 crystallized at $T_c = 110$ °C, the I_{1749} value still increases with temperature before the dominant melting, suggesting that besides the melting of the original α-form crystal, the α′- to α-crystalline phase transition also takes place in the temperature region corresponding to the endotherm P_2 in Figure 6a. As regards PLLA15 crystallized at $T_c = 120$ and 140 °C, the I_{1749} value does almost not change during the heating process, indicating that only the α-form crystal is developed in this case. Therefore, at 120 °C $< T_c <$ 130 °C, the double endotherms shown in Figure 6a are most likely due to the melting of the original and recrystallized α-form crystal, respectively. At $T_c > 130$ °C, the as-produced

α-form crystal is perfect enough, and it melts directly without the melt−recrystallization process, resulting in only one endotherm in the DSC curve.

In a word, the T_c-dependent melting of low- and high-MW PLLA is very similar. As for PLLA crystallized at low T_c, the α′- to α-crystalline phase transition takes place before the dominant melting. As regards the samples produced at high T_c, like the non-polymorphous polymers, the melting is in the melt−recrystallization mechanism or the direct melting of the perfect crystal. For the samples crystallized at middle T_c (100−120 °C), the transition of α′-form crystal and the melt of original α-form crystal take place synchronously before the melting of the α-form crystal formed in the previous phase transformation and melt−recrystallization processes.

Conclusions

In the present report, the effect of molecular weight on the polymorphous crystallization and melting behavior were investigated for PLLA with different MWs by DSC, POM, WAXD, and FTIR. It was found that, rather than the crystalline structure, the crystallization kinetics are quite dependent on the MW of PLLA. With increasing MW, the crystallization rate drops greatly. For both the low- and high-MW PLLA, the α′- and α-form crystals are produced at low and high T_c, respectively.

Moreover, the melting of PLLA is found to be also greatly influenced by T_c and MW. As for PLLA crystallized at low T_c, the transition from disordered α′-form crystal to ordered α-form crystal prior to the dominant melting was confirmed. In the high-MW PLLA crystallized at low T_c, almost all the α′-form crystals transform into the α-one in the heating scan. In contrast, as for the low-MW PLLA crystallized at low T_c, the α′-form crystals only partially transform into the α-one, and some amounts of α′-form crystals melt directly without transition during the heating process. With the increase of T_c, the melting of PLLA with various MWs changes from the phase transition + melting mechanism to the usual melt−recrystallization mechanism. Through this study, the T_c- and MW-dependent crystallization and melting behavior of PLLA were clarified, and the effects of T_c and MW on the polymorphism are quite important to interpret the peculiar thermal behavior of PLLA as well as for controlling the physical properties of PLLA by optimizing the crystallization process.

Acknowledgment. We thank Prof. Minoru Sakurai for the use of FTIR instrument, and we also thank Dr. Kazue Ueda and Unitika Co. Ltd. (Kyoto, Japan) for kindly supplying the PLLA samples.

References and Notes

(1) (a) Drumright, R. E.; Gruber, P. R.; Henton, D. E. *Adv. Mater.* **2000**, *12*, 1841. (b) Sinclair, R. G. *Pure Appl. Chem.* **1996**, *A33*, 585.

(2) (a) De Santis, P.; Kovacs, J. *Biopolymers* **1968**, *6*, 299. (b) Hoogsteen, W.; Postema, A. R.; Pennings, A. J.; Ten Brinke, G.; Zugenmaier, P. *Macromolecules* **1990**, *23*, 634. (c) Kobayshi, J.; Asahi, T.; Ichiki, M.; Okikawa, A.; Suzuki, H.; Watanabe, T.; Fukada, E.; Shikinami, Y. *J. Appl. Phys.* **1995**, *77*, 2957. (d) Sasaki, S.; Asakura, T. *Macromolecules* **2003**, *36*, 8385.

(3) (a) Eling, B.; Gogolewski, S.; Pennings, A. J. *Polymer* **1982**, *23*, 1587. (b) Puiggali, J.; Ikada, Y.; Tsuji, H.; Cartier, L.; Okihara, T.; Lotz, B. *Polymer* **2000**, *41*, 8921. (c) Sawai, D.; Takahashi, K.; Sasashige, A.; Kanamoto, T.; Hyon, S. H. *Macromolecules* **2003**, *36*, 3601. (d) Brizzolara, D.; Cantow, H. J.; Diederichs, K.; Keller, E.; Domb, A. J. *Macromolecules* **1996**, *29*, 191.

(4) (a) Cartier, L.; Okihara, T.; Ikada, Y.; Tsuji, H.; Puiggali, J.; Lotz, B. *Polymer* **2000**, *41*, 8909. (b) Zhang, J. M.; Duan, Y.; Sato, H.; Tsuji, H.; Noda, I.; Yan, S.; Ozaki, Y. *Macromolecules* **2005**, *38*, 8012.

(5) Lee, J. K.; Lee, K. H.; Jin, B. S. *Eur. Polym. J.* **2001**, *37*, 907.

(6) (a) Krikorian, V.; Pochan, D. J. *Macromolecules* **2005**, *38*, 6520. (b) Krikorian, V.; Pochan, D. J. *Macromolecules* **2004**, *37*, 6480. (c) Miyata, T.; Masuko, T. *Polymer* **1997**, *38*, 4003. (d) Cho, T. Y.; Strobl, G. *Polymer* **2006**, *47*, 1036. (e) Wang, Y.; Mano, J. F. *Eur. Polym. J.* **2005**, *41*, 2335. (f) Tsuji, H.; Miyase, T.; Tezuka, Y.; Saha, S. K. *Biomacromolecules* **2005**, *6*, 244. (g) Vasanthakumari, R.; Pennings, A. J. *Polymer* **1983**, *24*, 175. (h) Aou, K.; Kang, S.; Hsu, S. L. *Macromolecules* **2005**, *38*, 7730.

(7) (a) Abe, H.; Kikkawa, Y.; Inoue, Y.; Doi, Y. *Biomacromolecules* **2001**, *2*, 1007. (b) Di Lorenzo, M. L. *Eur. Polym. J.* **2005**, *41*, 569.

(8) (a) Ohtani, Y.; Okumura, K.; Kawaguchi, A. *J. Macromol. Sci., Part B: Phys.* **2003**, *3*−*4*, 875. (b) Yasuniwa, M.; Tsubakihara, S.; Iura, K.; Ono, Y.; Dan, Y.; Takahashi, K. *Polymer* **2006**, *47*, 7554.

(9) (a) Yamamoto, Y.; Inoue, Y.; Onai, T.; Doshu, C.; Takahashi, H.; Uehara, H. *Macromolecules* **2007**, *40*, 2745. (b) De Rosa, C.; Auriemma, F.; Vinti, V.; Galimberti, M. *Macromolecules* **1998**, *31*, 6206. (c) Woo, E. M.; Sun, Y. S.; Yang, C. P. *Prog. Polym. Sci.* **2001**, *26*, 945. (d) Cheng, S. Z. D.; Cho, M. Y.; Wunderlich, B. *Macromolecules* **1986**, *19*, 1868. (e) Wang, Z. G.; Hsiao, B. S.; Sauer, B. B.; Kampert, W. G. *Polymer* **1999**, *40*, 4615.

(10) (a) Gan, Z. H.; Kuwabara, K.; Abe, H.; Iwata, T.; Doi, Y. *Biomacromolecules* **2004**, *5*, 371. (b) Xu, J.; Guo, B. H.; Yang, R.; Wu, Q.; Chen, G. Q.; Zhang, Z. M. *Polymer* **2002**, *43*, 6893. (c) Yasuniwa, M.; Satou, T. *J. Polym. Sci., Part B: Polym. Phys.* **2002**, *40*, 2411.

(11) (a) Di Lorenzo, M. L. *J. Appl. Polym. Sci.* **2006**, *100*, 3145. (b) Ling, X.; Spruiell, J. E. *J. Polym. Sci., Part B: Polym. Phys.* **2006**, *44*, 3200.

(12) (a) Kister, G.; Cassanas, G.; Vert, M. *Polymer* **1998**, *39*, 267. (b) Zhu, B.; He, Y.; Asakawa, N.; Yoshie, N.; Nishida, H.; Inoue, Y. *Macromolecules* **2005**, *38*, 6445.

(13) (a) Acierno, S.; Grizuti, N.; Winter, H. H. *Macromolecules* **2002**, *35*, 5043. (b) Zhu, B.; He, Y.; Asakawa, N.; Nishida, H.; Inoue, Y. *Macromolecules* **2006**, *39*, 194. (c) Chen, H. L.; Li, L. J.; Ou-Yang, W. C.; Hwang, J. C.; Wong, W. Y. *Macromolecules* **1997**, *30*, 1718. (d) Rueda, D. R.; García Gutiérrez, M. C.; Ania, F.; Zolotukhin, M. G.; Baltá Calleja, F. J. *Macromolecules* **1998**, *31*, 8201. (e) Medellín-Rodríguez, F. J.; Larios-Lopez, L.; Zapata-Espinoza, A.; Davalos-Montoya, O.; Phillips, P. J.; Lin, J. S. *Macromolecules* **2004**, *37*, 1799. (f) Alamo, R. G.; Kim, M. H.; Galante, M. J.; Isasi, J. R.; Mandelkern, L. *Macromolecules* **1999**, *32*, 4050.

(14) Hoffman, J. D.; Weeks, J. J. *J. Res. Natl. Bur. Stand. (U.S.)* **1962**, *A66*, 13.

(15) Fox, T. G.; Flory, P. J. *J. Polym. Sci.* **1954**, *14*, 315.

(16) (a) Aou, K.; Hsu, S. L. *Macromolecules* **2006**, *39*, 3337. (b) Kang, S.; Hsu, S. L.; Stidham, H. D.; Smith, P. B.; Leugers, M. A.; Yang, X. *Macromolecules* **2001**, *34*, 4542.

MA071258D